
*Time-Frequency Methodology for Newborn
Electroencephalographic Seizure Detection*

Boualem Boashash and Mostefa Mesbah
Queensland University of Technology

CONTENTS

9.1	Introduction	339
9.2	Seizure Criteria and Time-Frequency Methodology	342
9.3	Seizure Patterns	353
9.4	Electroencephalogram Background Patterns	357
9.5	Time-Frequency Matched Detector	359
9.6	Discussion and Conclusions	366
	Acknowledgments	367
	References	367

9.1 Introduction

Techniques previously designed for electroencephalographic (EEG) seizure detection in the newborn have been relatively inefficient due to their incorrect assumption of local stationarity of the EEG. To overcome the problem raised by the proven nonstationarity of the EEG signal, current methods are extended to a time-frequency (TF) approach [8, 10]. This allows the analysis and characterization of the different newborn EEG patterns, the first step toward an automatic TF seizure detection and classification. An in-depth analysis of the previously proposed autocorrelation and spectrum seizure detection techniques identified the detection criteria that can be readily extended to the TF domain. We present the various patterns of observed TF seizure signals and relate them to current specialist knowledge of seizures. In particular, initial results indicate that a quasilinear instantaneous frequency (IF) can be used as a critical feature of the EEG seizure characteristics. These findings led to propose a TF-based seizure detector. This detector performs a two-dimensional (2D) correction between the EEG signal and a reference template selected as a model of the EEG seizure in TF domain.

9.1.1 Seizures and the electroencephalographic signal

Seizure may be the most frequent, and often the only, clinical sign of central nervous system dysfunction in the neonate [34]. Unlike adult seizure, the clinical manifestations of newborn seizure are subtle and hence require the constant attention of a medical specialist for diagnosis.

EEG has become a successful means of seizure detection in adults. This usually involves identifying sharp repetitive waveforms that indicate the onset of seizure. In adults, these EEG seizures are easily recognizable against a low amplitude random background characteristic of normal brain activity. The problem of detecting seizure in newborn babies, however, is complicated by a number of factors [28]. First, healthy newborn EEG signals representing normal brain activity often contain patterns such as spurious waveforms and sharp spikes. These characteristics, which would otherwise be detected as seizure in adults, are simply the result of extra electrical activity produced by the immature brain as it continues to form. Seizures, however, still usually appear in the EEG data as repetitive waveforms and the problem lies in discerning the healthy spikes from those formed from seizures. Second, visual symptoms of seizure, such as muscle spasms, rapid eye movement and drooling, are much subtler in newborns and may be easily missed. These visual indicators are also natural movements common to all newborn babies. Third, physical activity of babies in the intensive care environment is often subdued by medication to prevent injuries caused by unpredictable movements. This also reduces the chance of seizure detection using visual signs altogether. For these reasons, the EEG may be the only alternative for seizure detection in newborn.

9.1.2 Nonstationary and multicomponent characteristics of the electroencephalogram

There are three published methods for EEG seizure detection in newborns. The technique of Roessgen, Zoubir and Boashash [28] is a parametric approach based on a nonlinear estimation of 11 model parameters for detection. The two other methods are nonparametric. The spectrum technique introduced by Gotman et al. [16] uses frequency analysis to determine the changes in the dominant peak of the spectrum of short epochs of EEG data. The autocorrelation technique introduced by Liu [20] performs analysis in the time domain using short epochs of EEG data.

All three techniques are based on the assumption that the EEG signals are locally stationary. However, a closer examination of these signals clearly shows that they exhibit significant nonstationary and multicomponent features [9, 24] (Figure 9.1). Therefore, the basic assumption on which these three methods are based is essentially invalid and at best only an approximation.

To take this fact into account, we extend the autocorrelation and spectrum techniques to the nonstationary case by introducing both time variation and frequency variation parameters in the basic equations on which these techniques are based. This extension leads to a TF formulation in the $(t - f)$ domain or a time-varying autocorrelation formulation in the time-lag domain $(t - \tau)$.

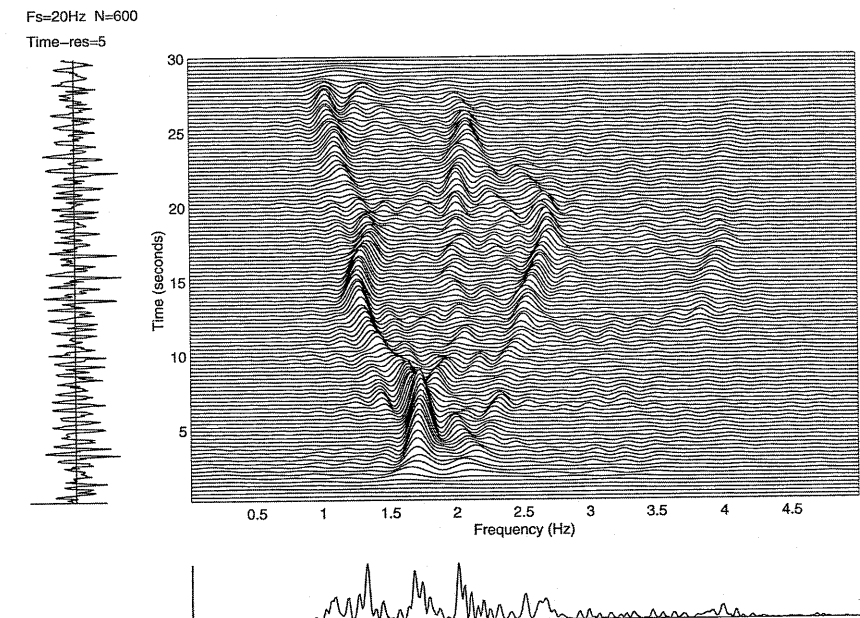


FIGURE 9.1

Time-frequency (TF) representations of newborn EEG seizure signal using the B distribution. This EEG clearly shows the multicomponent and nonstationary nature of the seizure.

Having taken into account the nonstationary aspect of the EEG signals, we still need to deal with the other aspect, namely, the multicomponent behavior. This requires a selection of an appropriate time-frequency distribution (TFD) that is capable of handling multicomponent signals. Once this has been done, a calibration process is undertaken to translate the seizure criteria from the spectrum and autocorrelation domains to the TF domain. This initially involves the reproduction of the seizure detection criteria used by the two previously mentioned methods and map them in a joint TF domain. Features in the joint $t - f$ domain characterizing seizure are then identified and a detection process based on those features is constructed and tested. Once we have a better understanding of the processes involved for each method and determined which components are most suited to a TF representation, we combine them in a TF-based detection process as illustrated in Figure 9.2.

9.1.3 Electroencephalographic acquisition

The electrical signals produced in the brain are monitored in a noninvasive manner by measuring variations in potential on the scalp. The EEG signals are measured using strategically placed small electrodes on the scalp. One electrode, usually at the base of the skull, acts as a reference (ground) signal, and various channels of data are

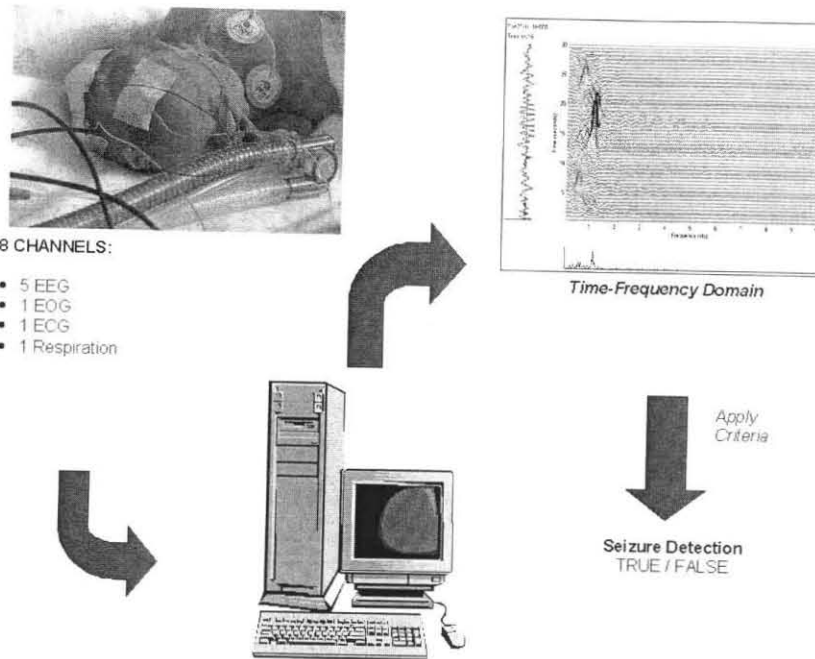


FIGURE 9.2

TF-based seizure detection process.

created by measuring the voltage differences between neighboring electrodes. Due to the size of most newborn babies' heads, only 5 channels of EEG have been recorded in each session using the 10 to 20 International System of Electrode Placement. The sampling rate used for recording the EEG data was 256 Hz. For the sake of artifact detection, three auxiliary signals representing electro-oculogram (EOG), electrocardiogram (ECG) and respiration were also recorded. Data used in this study were collected at the Royal Women's Hospital Perinatal Intensive Care Unit in Brisbane, Australia.

9.2 Seizure Criteria and Time-Frequency Methodology

9.2.1 Basic definitions and relationships

The autocorrelation function of a random nonstationary process $x(t)$ may be written as:

$$R_x(t, \tau) = E[x(t)x(t + \tau)] \quad (9.1)$$

where τ represents a time difference, or lag and E is the expectation operator. If the process is at least wide-sense stationary (WSS), the autocorrelation function becomes simply a function of τ , that is:

$$R_x(t, \tau) = R_x(\tau) \quad (9.2)$$

For the case of stationary signals, Wiener–Khintchine theorem states that the power spectral density of $x(t)$ can be obtained by simply taking the Fourier transform (FT) of Equation (9.2). In other words:

$$S_x(f) = \text{FT}_{\tau \rightarrow f}\{R_x(\tau)\} \quad (9.3)$$

where $R_x(\tau)$ is defined in Equation (9.2). This equation is valid only for stationary signals. For the case of nonstationary signals, Equation (9.3) gives averaged values over the variations of the signal spectral contents and thus significant information may be lost.

For nonstationary signals, the Wiener–Khintchine theorem can be extended so that the time-varying power spectral density $S_x(t, f)$ of a signal $x(t)$ is also related to the time-varying autocorrelation function $R_x(t, \tau)$ of the same signal by the following FT relation:

$$S_x(t, f) = \text{FT}_{\tau \rightarrow f}\{R_x(t, \tau)\} \quad (9.4)$$

or more explicitly:

$$S_x(t, f) = \int_{-\infty}^{\infty} R_x(t, \tau) e^{-j2\pi f \tau} d\tau \quad (9.5)$$

The expression $S_x(t, f)$ given by Equation (9.5) reduces to the Wigner–Ville spectrum [5]. For practical reasons, $x(t)$ is replaced by its analytical associate $z(t)$. Estimates of $S_z(t, f)$ can be expressed by the quadratic class of TFDs [5]:

$$\rho_z(t, f) = W_z(t, f) \ast \gamma(t, f) \quad (9.6)$$

where $\gamma(t, f)$ is a 2-D kernel window that is application dependent, $W_z(t, f)$ is the Wigner–Ville distribution (WVD) of $z(t)$, and \ast indicates a double convolution in both time and frequency. By expanding Equation (9.6), we obtain [5]:

$$\rho_z(t, f) = \int_{-\infty}^{\infty} \int_{-\infty}^{\infty} \int_{-\infty}^{\infty} g(\nu, \tau) z(u + \tau/2) z^*(u - \tau/2) e^{j2\pi(\nu t - \nu u - f \tau)} du d\nu d\tau \quad (9.7)$$

where the superscript $*$ stands for complex conjugate. The kernel filter $g(\nu, \tau)$ characterizes a particular TF distribution and is related to $\gamma(t, f)$ via a double Fourier transformation. Equation (9.7) is the general formulation of the quadratic class of

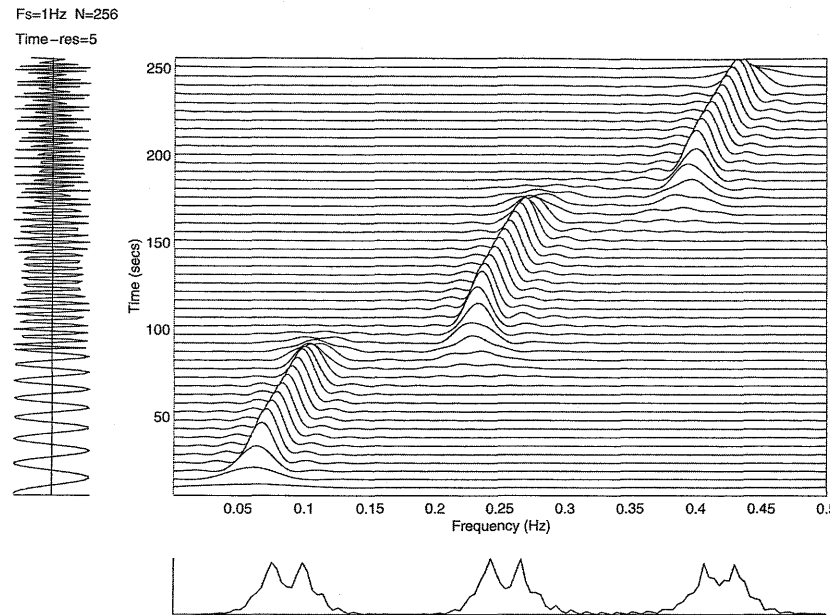


FIGURE 9.3

TF representation of a three-component signal.

TFDs in terms of the Doppler-lag kernel $g(\nu, \tau)$ [6]. The TFD $\rho_z(t, f)$ can be further expressed in the following form:

$$\rho_z(t, f) = \int_{-\infty}^{\infty} \int_{-\infty}^{\infty} G(t-u, \tau) z(u + \tau/2) z^*(u - \tau/2) e^{-j2\pi f \tau} du d\tau \quad (9.8)$$

where $G(t, \tau)$ is the inverse FT of filter kernel $g(\nu, \tau)$. A shorter version of Equation (9.8) is given by:

$$\rho_z(t, f) = \text{FT}_{\tau \rightarrow f} \{ K_z(t, \tau)^* G(t, \tau) \} \quad (9.9)$$

where $K_z(t, \tau) = z(t + \tau/2) z^*(t - \tau/2)$ is the signal kernel. This equation leads to the easiest discrete-time version of TFDs for implementation purpose [5].

A typical TF plot of a nonstationary multicomponent frequency-modulated (FM) signal is shown in Figure 9.3. The representation on the left is the time-domain representation. From this representation we observe that the signal significantly changes its periodicity characteristics at time $t = 100$ sec and time $t = 175$ sec. The representation at the bottom is the magnitude spectrum of the signal. It shows that this signal consists of three disjoint frequency bands. The main plot is the TF representation of the same signal. It not only combines the information from both time and frequency representations but also preserves the phase information, disregarded

or unavailable in the other two representations. This allows the joint TF representation to clearly show that the signal consists of three components characterized by:

1. Frequency 0.05 to 0.1 Hz during time $t = 0$ to 100 sec
2. Frequency 0.25 to 0.3 Hz during time $t = 100$ to 175 sec
3. Frequency 0.4 to 0.45 Hz during time $t = 175$ to 250 sec

The TF representation shows not only the number of components present in the signal but also how they vary in time and frequency, when they start and finish and whether they coexist at the same time or same frequency. For this particular example, the TF representation indicates the linear FM nature of all three components, which cannot be deduced from either time or frequency representations only.

9.2.2 Time-frequency distribution selection

The EEG data collected thus far show that neonatal EEG seizures are highly nonstationary and occasionally multicomponent, and are mostly concentrated in the band of frequency (0 to 5) Hz [8–10]. These factors must be taken into account when selecting an optimal TFD, because each TFD is more suited to representing signals with particular characteristics. For example, the WVD is known to be optimal for monocomponent linear FM signals but performs poorly for multicomponent or highly nonlinear FM signals.

Because neonatal EEG signals are nonstationary and occasionally multicomponent, the selected TFD needs to have good spectral resolution and reduced cross terms. For this sake, the performances of several distributions have been compared to find an optimal TF representation of real neonatal EEG data. The comparison study included the spectrogram, Wigner–Ville (WV), Choi–Williams (CW), B (BD), Zalto–Atlas–Marks (ZAM), Born–Jordan (BJ) and Rihaczek–Margenau distributions [8]. The performances of the resulting TFDs have been compared using an objective quantitative measure criterion [7]. Based on this criterion along with extensive experimental results, the B distribution BD with the smoothing parameter β equals to 0.01 — see Equation (9.10) — has been found to be the most suitable TF representation of the newborn EEG. The BD is defined in terms of its time-lag kernel — see Equation (9.8) — which is given by:

$$G(t, \tau) = \left(\frac{|\tau|}{\cosh^2(t)} \right)^\beta \quad (9.10)$$

where β ($0 < \beta \leq 1$) is a parameter that controls the sharpness of the cutoff of the 2D filter in the time-lag domain (t, τ) . Figure 9.4 shows the TFDs of a 30-sec sample of real newborn EEG data using the B, CW, ZAM and WV distributions and clearly illustrates the superiority of B distribution in terms of resolution and cross-term reduction.

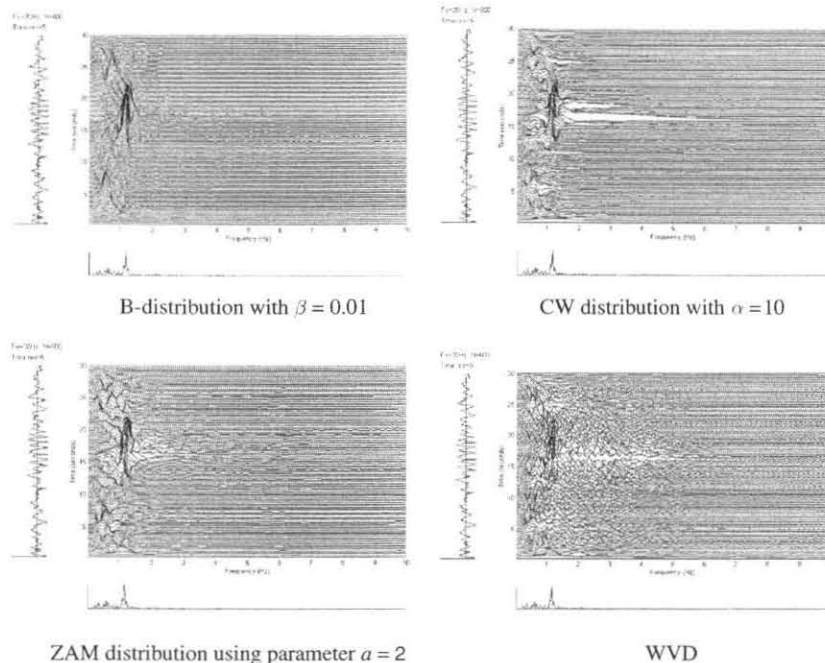


FIGURE 9.4

TF representations of a real epoch of newborn EEG using different TFDs.

9.2.3 From time domain to time-frequency domain

Seizure detection using the autocorrelation method relies on the assumption that the essential characteristic in newborn seizure EEG is periodicity. The periodicity of the autocorrelation of short epochs of EEG data is quantified (scored) using a nonlinear rule-based algorithm. In this technique, an epoch consisting of 30 sec of data is divided into 5 windows (see Figure 9.5). Depending on the autocorrelation function of each window, up to four primary periods (T_1, \dots, T_4) are calculated for each window in an epoch as shown in Figure 9.6. These times correspond to the moment centers of the first four peaks of the autocorrelation function. The windows are then scored whereby more evenly spaced primary periods are allocated larger scores. After each window in an epoch is scored, a second rule-based scheme is used to classify each epoch as positive or negative. If an epoch is classified as positive in two or more channels, this epoch is considered to contain seizure [20].

9.2.3.1 Seizure criteria for the autocorrelation method

A single window is declared as seizure positive by the autocorrelation method if the following criteria are met [8]:

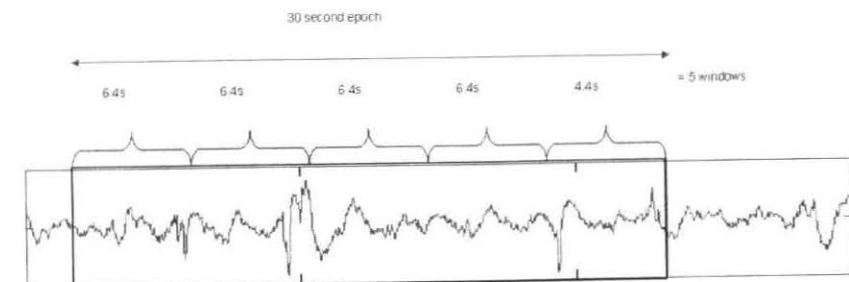


FIGURE 9.5

Epoch and window definitions according to the autocorrelation method.

1. At least four periods exist within the positive half of the autocorrelation function.
2. The differences between the ratios of each moment center to the first and the nearest integer are less than 0.150.
3. The total score obtained by summing all moment center scores is greater than or equal to 12 (out of a maximum of 15).

9.2.3.2 Mapping of autocorrelation seizure criteria to time-frequency domain

An EEG signal within a given window is considered seizure if in the TF domain a continuous spectral peak exists within that window and meets the following criteria:

1. All frequencies within the spectral line are greater than 0.625 Hz within 6.4-sec windows or greater than 0.909 Hz within 4.4-sec windows.

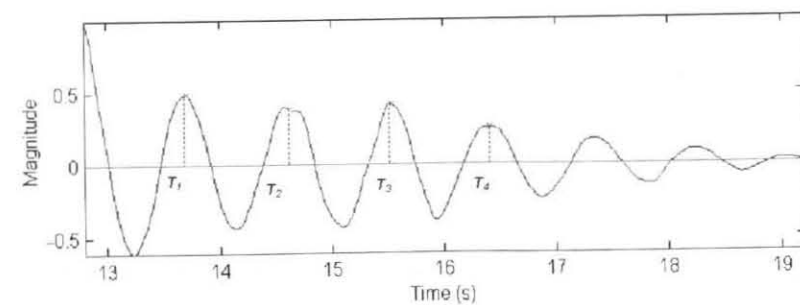


FIGURE 9.6

Autocorrelation function for one window.

2. The length of continuous dominant spectral peak within the window is greater than 3 sec.

A continuous spectral peak is defined as adjoining peaks within the TF array above a selected threshold of one fifth the maximum array value. The threshold was chosen experimentally.

Criterion 1 is a direct translation to the frequency domain of the first criterion described earlier in the autocorrelation domain. The second criterion has been deduced by observing several TF representations of seizure positive windows as defined by the autocorrelation method. The scoring system proposed by the autocorrelation method focuses on identifying periodic regions of data in the lag domain. Periodic regions are clearly identified in TF representations by a dominant spectral peak occurring for a certain time interval.

9.2.3.3 Results and discussion

Extraction of the seizure criteria listed earlier in the TF domain has been successfully calibrated with the autocorrelation method. Peak detection techniques have been employed to simplify the extraction process, resulting in a detection array illustrating positions and lengths of continuous spectral lines within each epoch. Figure 9.7 shows the algorithm flowchart used in the calibration of this method.

Good results have been obtained using TF algorithm to detect individual seizure windows of real neonatal EEG in the TF domain. Approximately 75% of windows detected as seizure positive by the autocorrelation method are detected using TF criteria listed earlier. The results of applying the TF-based detection method are summarized in Figure 9.8. In this figure, the original epoch refers to the raw TF array produced from preprocessed EEG data. Image of this array appears on the left side of the figure. The image is also divided into four distinct 6.4-sec windows and one 4.4-sec window as defined by the autocorrelation method. Window scores attributed to these windows are displayed at the end of each window division for easy comparison between the TF information and the corresponding score allocated by autocorrelation method.

9.2.4 From frequency domain to time-frequency domain

The spectrum analysis method has also been used to detect periodic discharges in the EEG signal. As shown in Figure 9.9, a background epoch is defined as a 20-sec segment of EEG finishing 60 sec before the start of the current 10-sec epoch under investigation. From the frequency spectrum of each 10-sec epoch, the following features are extracted: the frequency of the dominant spectral peak, the width of the dominant spectral peak and the ratio of the power in the dominant spectral peak to that of the background spectrum in the same frequency band.

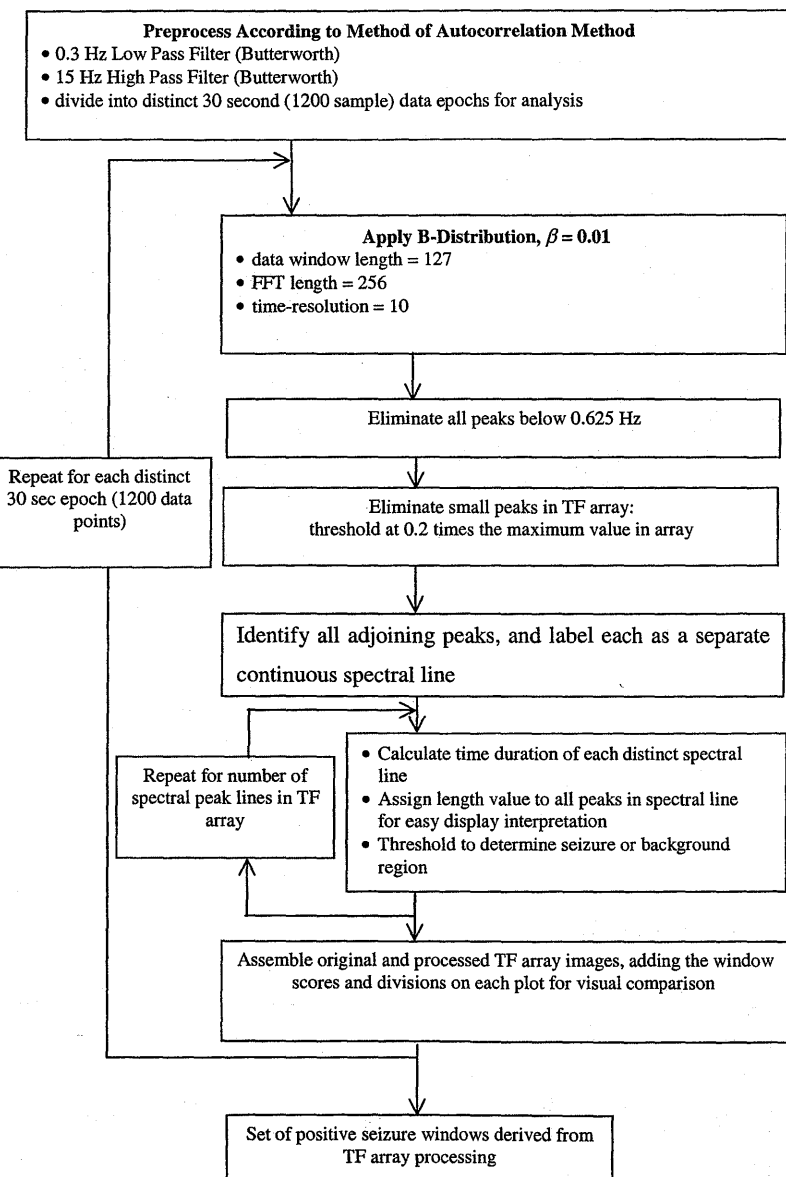


FIGURE 9.7

Implementation and calibration of the TF extension of time-domain method.

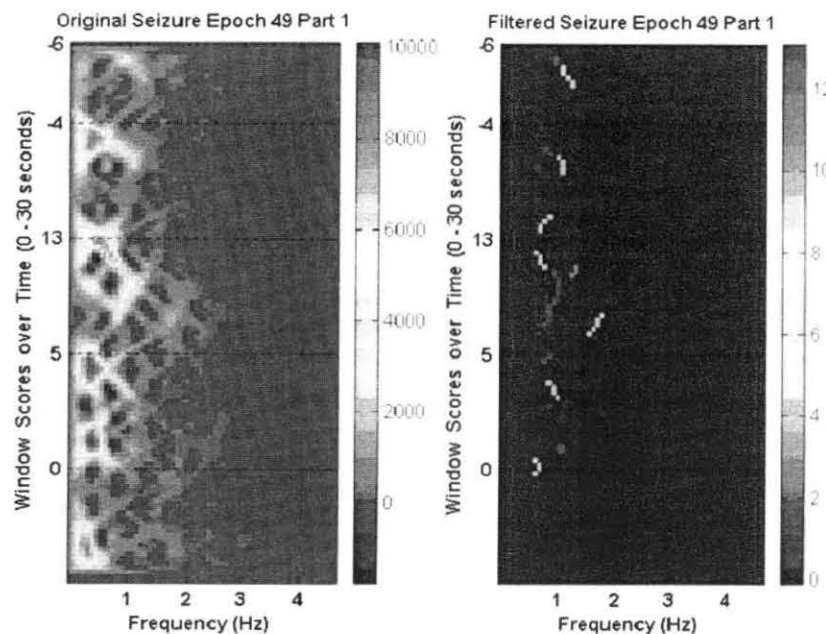


FIGURE 9.8

The mapping of the features from autocorrelation to TF. Seizure windows are defined by the presence of high value lines. As the length of each spectral line is denoted by its color, windows with dark lines should indicate scores higher or equal to 12.

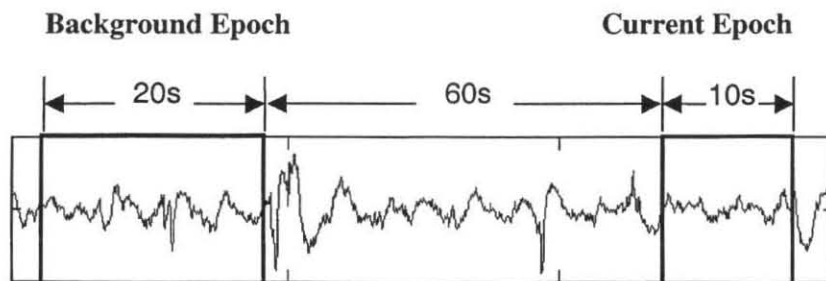


FIGURE 9.9

Epoch and window definitions according to the spectrum method.

9.2.4.1 Seizure criteria in the spectral domain

The 10-sec epoch of EEG data is considered seizure positive if any of the 3 following criteria are met [16]:

	Dominant Frequency	Maximum Bandwidth	Half-Power Ratio
Criterion 1	0.5–1.5 Hz	≤ 0.6 Hz	3–4
Criterion 2	1.5–10 Hz	≤ 0.6 Hz	2–4
Criterion 3	1.5–10 Hz	≤ 1 Hz	4–80

To limit the number of false alarms, a seizure detection is discounted if the epoch is largely nonstationary, if a large amount of alternating current (AC) power noise is present or if it appears that an EEG lead has been disconnected.

9.2.4.2 Mapping of spectrum criteria to time-frequency domain

The preceding criteria pertaining to frequency and bandwidth are clearly observable in the TF domain. That is, each spectra containing a dominant peak that meets either of the criteria:

1. Frequency in the range 0.5 to 1.5 Hz and width ≤ 0.6 Hz
2. Frequency in the range 1.5 to 10 Hz and width ≤ 1 Hz

may be considered for further seizure detection pertaining to power ratio. Disregarding the power ratio criteria, the second criterion given in the preceding table becomes a subset of the third criterion.

9.2.4.3 Results and discussion

The calibration of the two TF criteria identified earlier is illustrated in Figure 9.10. This essentially extracts frequency and width information, the results of which are visible in the plots shown in Figure 9.11 for a 30-sec epoch. Data are presented by highlighting the dominant frequency with a color indicating the width of the spectral peak. Boxed sections of the array indicate EEG regions detected as containing seizure by the conventional spectrum method.

9.2.5 Time-frequency patterns

Calibration of the TF method using both autocorrelation and spectrum method has been successfully performed. This calibration led to consideration of a fully integrated TF detection method by combining the different TF seizure features. The visual analysis of these EEG TF features indicates that there are two distinguishable classes of TF EEG patterns: seizure and background. Further, the seizure patterns can

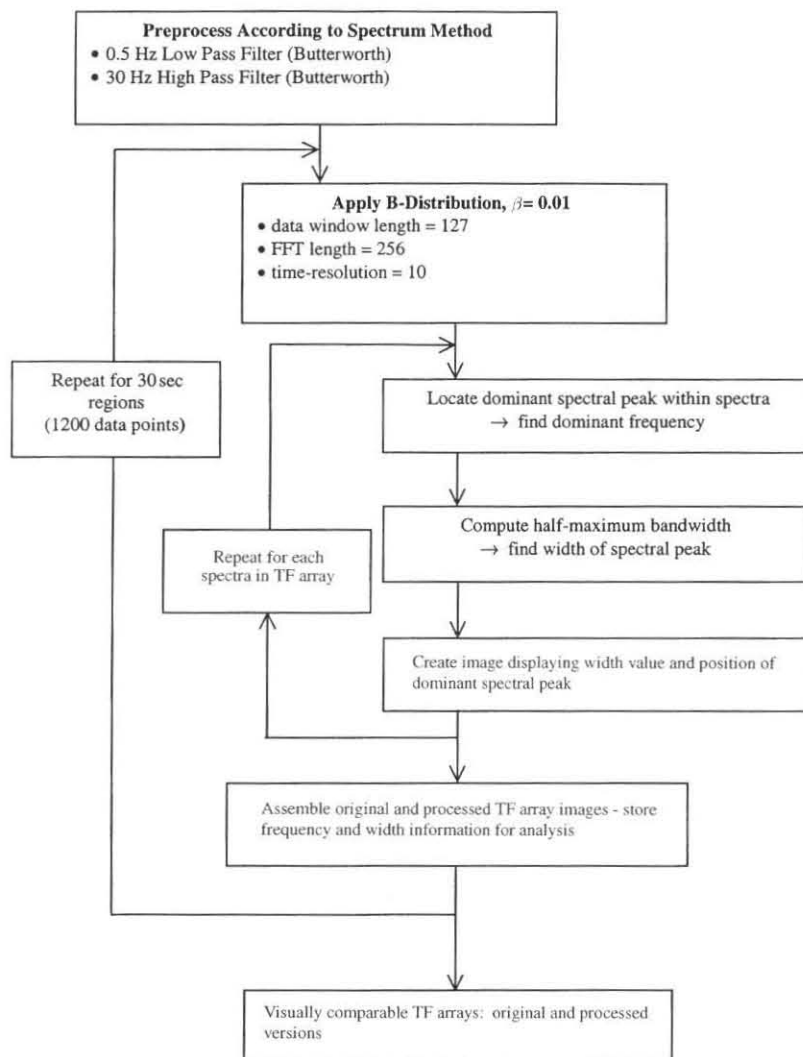


FIGURE 9.10

Implementation and calibration of TF extension of frequency-based method.

be characterized in terms of the dominant spectral peak as either a linear FM or a piecewise linear FM whereas the background patterns exhibit a low-frequency burst of activities or activities with no clearly defined pattern. These visual observations correlate well with the clinical information related to the different patterns found in

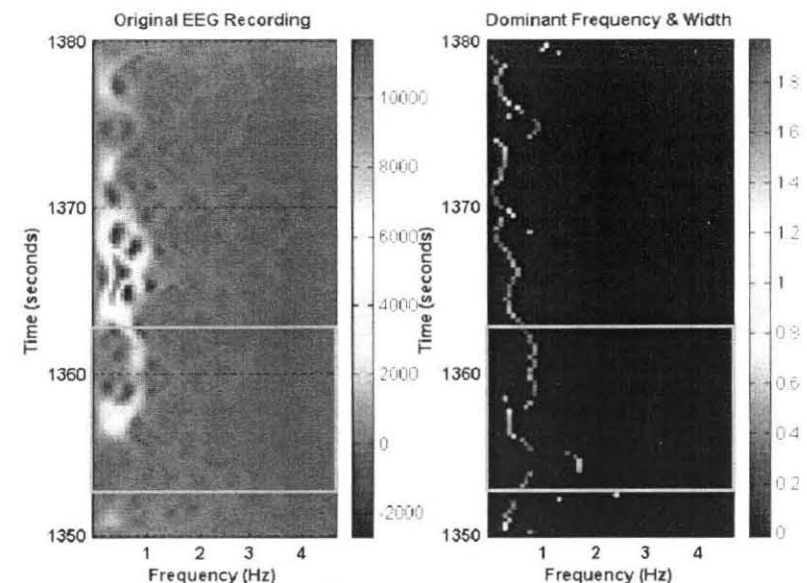


FIGURE 9.11

Mapping of the features from spectrum to TF. The color of the dominant frequency is related to the width of the spectral peak. Boxed sections indicate the presence of seizure as detected by the spectrum method.

EEG [21]. A few representative TF patterns that characterize each of the subclasses defined so far are given next.

9.3 Seizure Patterns

As mentioned earlier, the following patterns characterize the different patterns found thus far in the EEG signals in terms of dominant spectral peak.

9.3.1 Linear frequency-modulated patterns

A number of the EEG seizures analyzed in the TF domain can be approximated by linear FM (LFM) with either fixed or time-varying amplitudes. These patterns can be further classified into the following subclasses:

9.3.1.1 Class A (linear frequency-modulated patterns with a quasi-constant frequency)

Figure 9.12 shows a seizure that has a linear FM behavior with an almost constant frequency. The amplitude of the TF seizure pattern increases at the onset and decreases

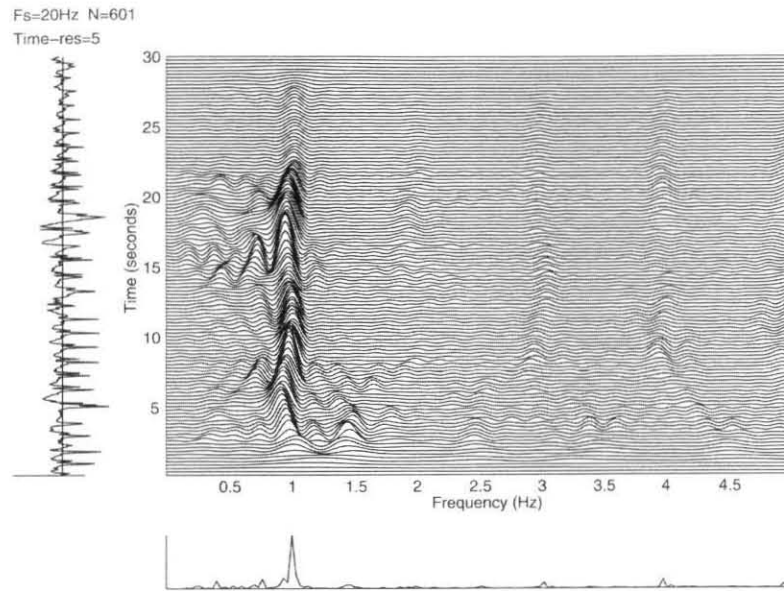


FIGURE 9.12

TF representation of a seizure that shows a linear FM behavior with constant frequency.

toward the end. These observations are in agreement with the seizure definition found in medical literature [21]. In this figure, we can clearly see the dominant peak (frequency domain) and the repetitive pattern of the spikes and sharp waves (time domain) characterizing the newborn seizures. A major advantage of the TF representation is that we can easily distinguish the seizure from the background. An interesting phenomenon that was observed is the existence of subharmonics in a number of TF representations of EEG seizure as illustrated in, for example, Figure 9.13. This characteristic of the newborn EEG seizure has also been reported by Lombroso [21].

9.3.1.2 Class B (short linear frequency-modulated patterns with a Quasi-constant frequency)

Figure 9.14 shows a seizure pattern that differs from those in class A in one important aspect, the duration. A disagreement exists between researchers about what constitutes a seizure. The duration of rhythmic discharges that characterizes a seizure is highly variable, from as short as 1 sec to as long as 30 min [25]. To consider an EEG signal as a seizure, some researchers require that it must last at least 10 sec [12, 16]; others require a minimum of 20 sec [23], whereas a third group does not specify a time limit [19–21]. Due to this disagreement, these controversial seizures were classified as a separate category.

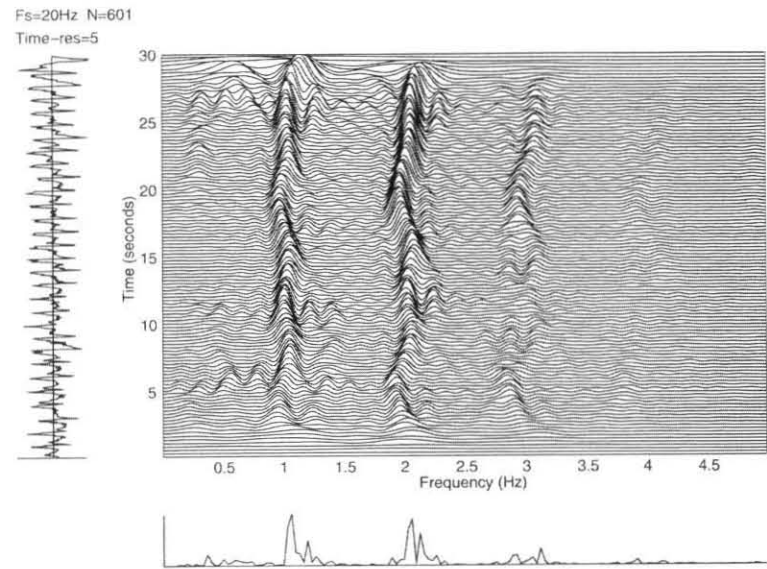


FIGURE 9.13

TF representation of a seizure that shows subharmonics.

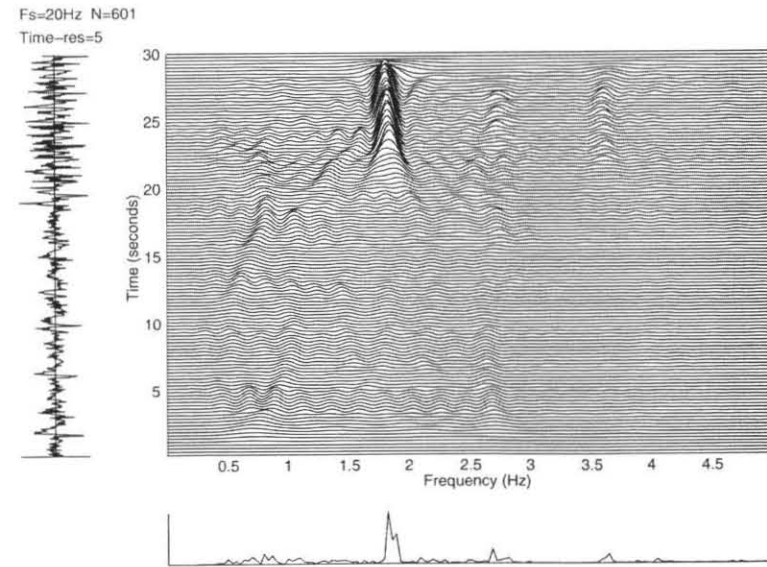


FIGURE 9.14

TF representation of a short duration harmonic discharge "seizure."

9.3.1.3 Class C (linear frequency-modulated patterns with a decreasing frequency)

Figure 9.15 of this class can be characterized by its IF that tends to decrease with time. This frequency-decreasing behavior is widely accepted as a characteristic of the EEG seizure [21, 29]. The advantage of the TF representation over those of the time or frequency is that the linear FM character is easily recognizable. A similar behavior can be seen in the work of Franaszczuk on adult seizures originating from the mesial temporal lobe during the periods of organized rhythmic activity [14].

9.3.2 Piecewise linear frequency-modulated patterns

A pattern of this class is shown in Figure 9.16. It can be approximated by piecewise linear FM. Something similar can be observed in one of the TF representations produced by Franaszczuk in his study of the adult seizure originating from the mesial temporal lobe [14].

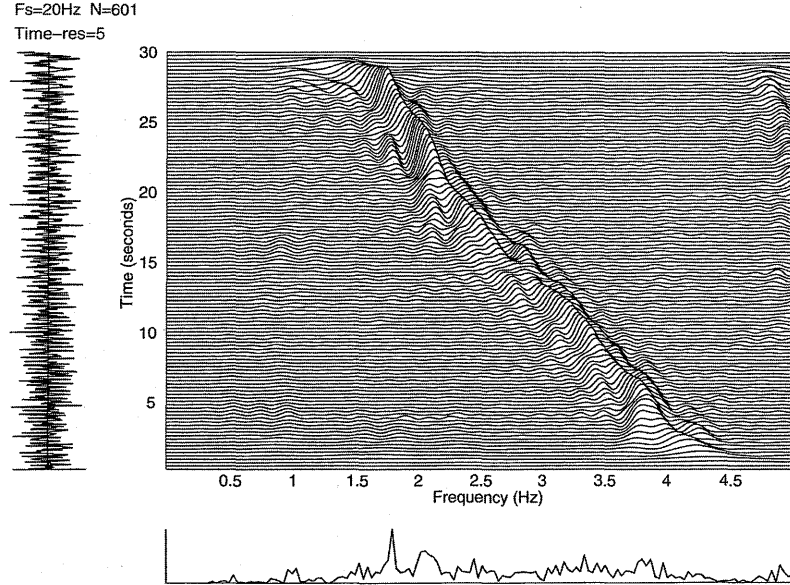


FIGURE 9.15

TF representation that shows an LFM behavior with decreasing frequency.

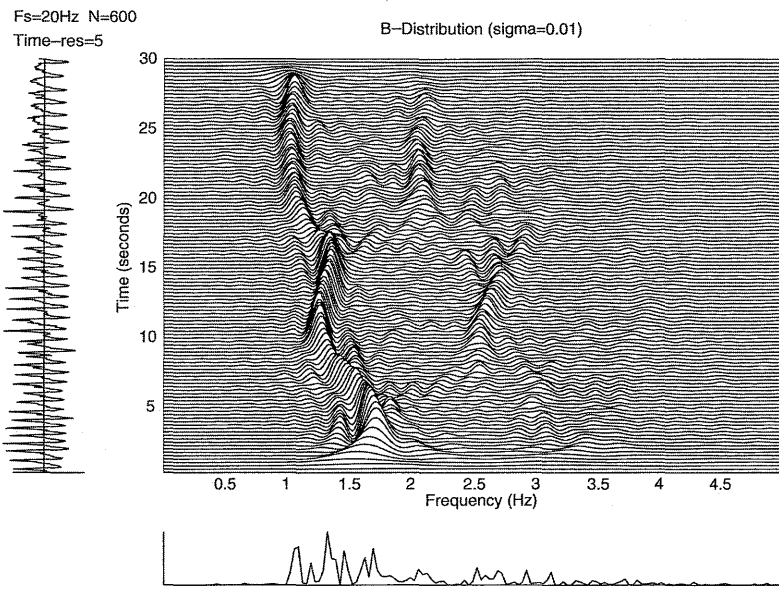


FIGURE 9.16

TF representation of an EEG seizure that shows a piecewise LFM behavior.

9.4 Electroencephalogram Background Patterns

By background, we mean any signal that is not classified as seizure. Two distinct patterns have been observed while analyzing the EEG signals: burst suppression activity and irregular activity with no clear pattern.

9.4.1 Class E (burst suppression)

Figure 9.17 is an example of this class. It shows instance of burst activities. These are short period signals with a high energy lasting for few seconds and usually occurring at frequencies below 8 Hz. These features are characteristic of burst suppression as defined in the literature. Burst suppression consists of burst of high voltage activity lasting 1 to 10 sec and composed of various patterns (δ [0 to 4 Hz] and θ [4 to 8 Hz] with superimposed and intermixed spikes, sharp waves and faster activity) followed by a marked background attenuation [29].

9.4.2 Class F (activities lacking a specific pattern)

Figure 9.18 is an example of EEG epochs lacking a well-defined and consistent pattern. These types of activities do not seem to be constrained within the low-frequency band characterizing the seizure signals.

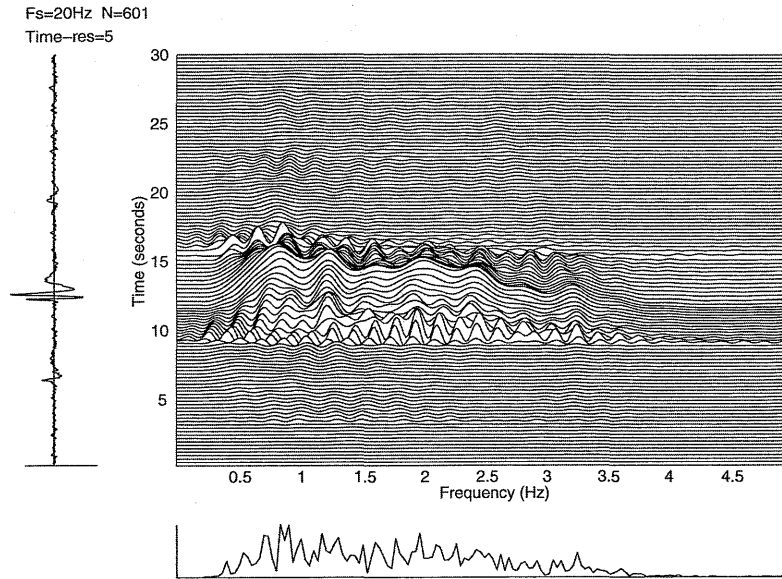


FIGURE 9.17

TF representation of burst suppression.

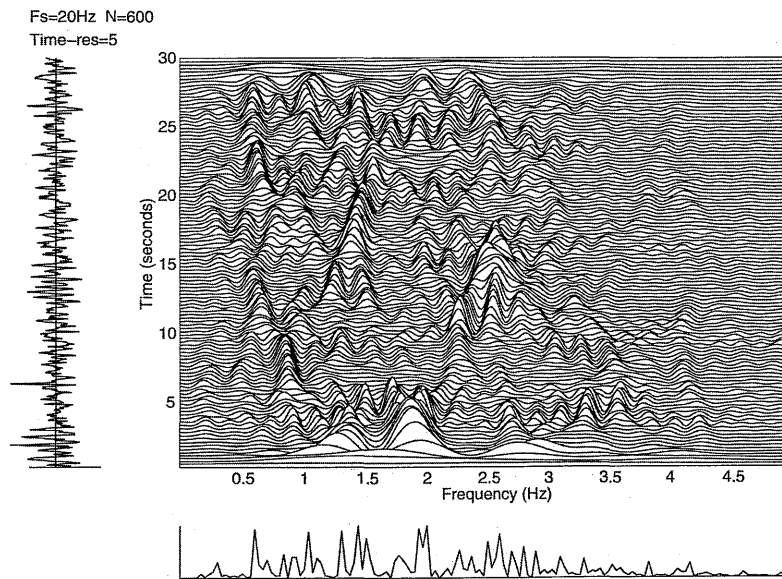


FIGURE 9.18

TF representation of an EEG lacking specific and consistent pattern.

9.5 Time-Frequency Matched Detector

The matched filter (which essentially reduces to a correlator receiver) is very popular for constructing detectors and classifiers. For known deterministic signals in white Gaussian noise (WGN), the correlator receiver is known to be optimal in the Neyman Pearson sense for detection [32] and in a Bayesian sense for classification [31]. To construct a detector, the output of a correlator is compared with a threshold. The threshold is chosen such that the probability of a false alarm is maintained.

Traditionally, the correlator receiver is implemented in time domain as a one-dimensional (1-D) correlation between the received noisy signal $x(t)$ and a reference signal $s(t)$. For random signals, this can be done using the corresponding spectral representations. To extend this detector to handle nonstationary signals, the 1-D correlation is replaced by a 2-D correlation involving the TF distribution of $x(t)$ and $s(t)$, as shown in Figure 9.19. The resulting test statistic is given by:

$$T(x) = \iint \rho_x(t, f) \rho_s(t, f) dt df \quad (9.11)$$

This type of detector has been implemented using different quadratic TF distributions such as the spectrogram [1, 33], the reassigned spectrogram [33], the WVD and cross-WVD [2–4, 13, 18, 30], and generalized time-shift covariant quadratic TFD [26–27]. It has also been implemented in the ambiguity domain by replacing the TFDs by the auto- and cross-ambiguity functions [33].

By using Moyal's formula [17], we get:

$$\iint \rho_x(t, f) \rho_s(t, f) dt df = \left| \int x(t) s^*(t) dt \right|^2 \quad (9.12)$$

This equality is only valid when the filter kernel $g(\nu, \tau)$ in Equation (9.8) is unimodular, that is:

$$|g(\nu, \tau)| = 1 \quad (9.13)$$

for all ν and τ .

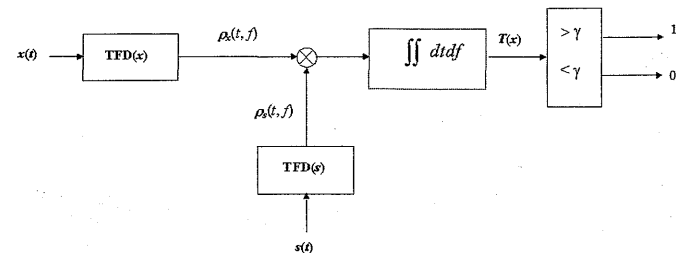


FIGURE 9.19

TF matched receiver.

This is the case, for example, for the WV, the Rihaczek [13] and the generalized time-shift quadratic TFDs [27]. Equation (9.12) is an alternative interpretation of the correlator receiver in terms of a correlation of the TFDs.

It has been shown [2, 13] that for the case of deterministic signal in noise (even WGN) that the TF-based correlator is suboptimal. This suboptimality can be partly explained by the nonlinearity of the quadratic TFDs that accentuates the effects of noise by introducing artifacts.

To use a correlator receiver, it is usually required that the wave shape of the reference signal (or other related information such as its TFD) as well as the noise statistics are known. For the case of EEG seizure detection, the wave shape of the EEG seizure is generally unknown. In Section 9.3, however, we have shown that the EEG seizure can be characterized by a linear or a piecewise linear FM. Based on this conclusion, we propose to construct a TF-based matched filter (i.e., essentially a correlator). To do this, a representative TF distribution of a linear FM $\rho_{ref}(t, f)$ is selected to serve as template (reference). The correlator statistic $T(z)$ used is the 2-D cross-correlation between the noisy signal and the reference signal TFDs [2], that is:

$$T(z) = \iint \rho_{ref}(t, f) \rho_z^*(t, f) dt df \quad (9.14)$$

where z is the analytical signal corresponding to the EEG signal to be analyzed..

9.5.1 Implementation of the time-frequency-matched detector

A working model of the TF-matched detector as shown in Figure 9.20 has been implemented. A description of its main components are described in the next section.

9.5.1.1 Preprocessing

This stage can include any preprocessing of the EEG signal collected from the newborn's scalp. Some major reasons for preprocessing the EEG signal include artifact (such as ECG, EOG and EMG) removal, noise filtering and resampling the signal to comply with detector input specifications. In the present implementation of this detector, the process of artifact removal has not been included.

9.5.1.2 Signal restructuring

Because it is neither desirable nor practical to work with a very long EEG signal, we found it necessary to segment the EEG into an array of signals of fixed length. After some preliminary testing, we found a length of 2 min to be suitable for performing the cross-correlation. Shorter signal lengths led to higher rates of miss detections and false alarms. Once the full input EEG signal is divided into blocks of 2-min duration, each block is stored as a row of the newly formed array of signals. In the development of this detector, a protocol of 50% overlap of each block was adopted, as displayed in Figure 9.21.

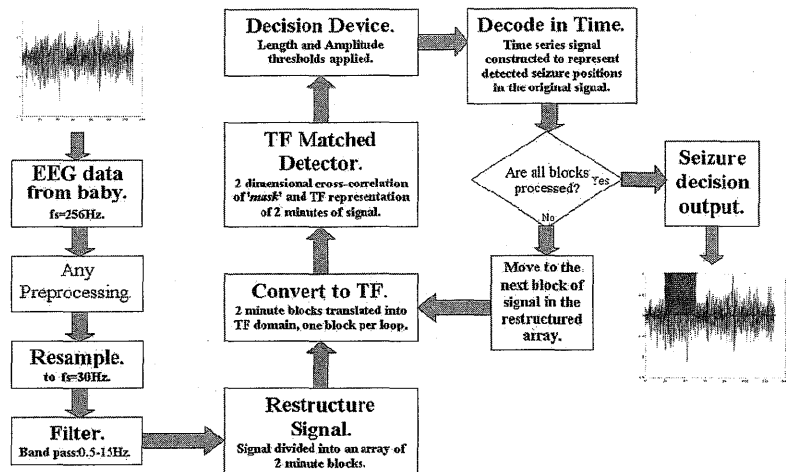


FIGURE 9.20

Block diagram of TF-matched detector.

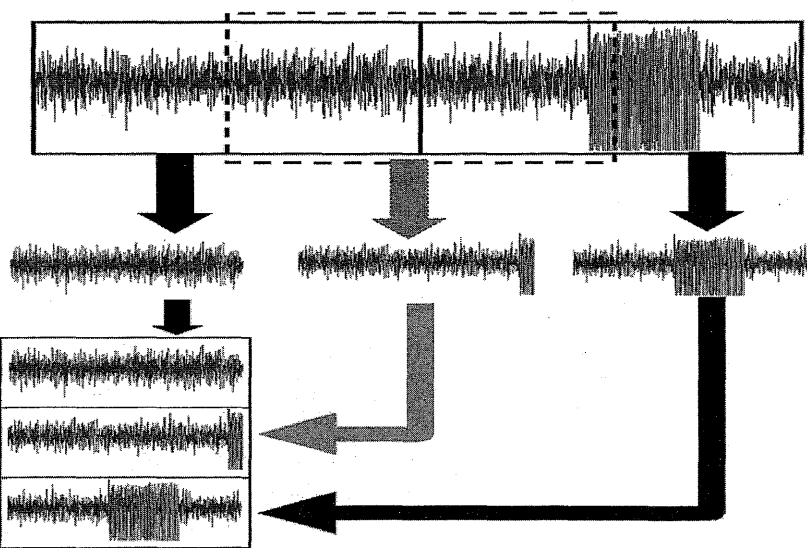


FIGURE 9.21

Segmenting the EEG signal in blocks of 2-min length.

9.5.1.3 Detection loop

The detection loop is executed until all the blocks of the input EEG signal have been processed. An offset value is maintained, giving a precise location in the original signal where abnormal events are detected.

9.5.1.4 Cross-correlation implementation

This forms the critical step in the effectiveness of this TF seizure detector. The cross-correlation between the input TF array and the template (mask) is obtained using the 2-D cross-correlation function given by Equation (9.14). The most crucial process is the choice of the template. This problem is discussed later. We found it convenient to normalize TF distributions of both the reference signal and the EEG signal.

9.5.1.5 Amplitude and length criteria

Ideally there would be one peak value in the output of the cross-correlation array, with its amplitude determining the presence or absence of seizure. This proved a little unreliable, and it was decided to search for a sequential series of values over the amplitude threshold. This proved very successful, and a minimum ridge length of 20 sec over the amplitude threshold was classed as a seizure. The 20-sec length adopted is larger than the minimum 10-sec length of EEG seizure adopted by many neurologists [12]. This length can be changed at will. An example of the correlation output, following the application of a threshold is shown in Figure 9.22, where the ridges of length equal or greater than 20 sec indicate the presence of seizure.

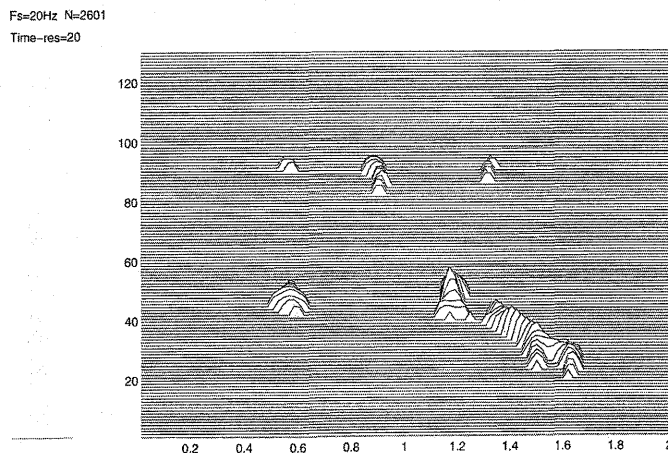


FIGURE 9.22

Amplitude threshold applied to output of the matched filter.

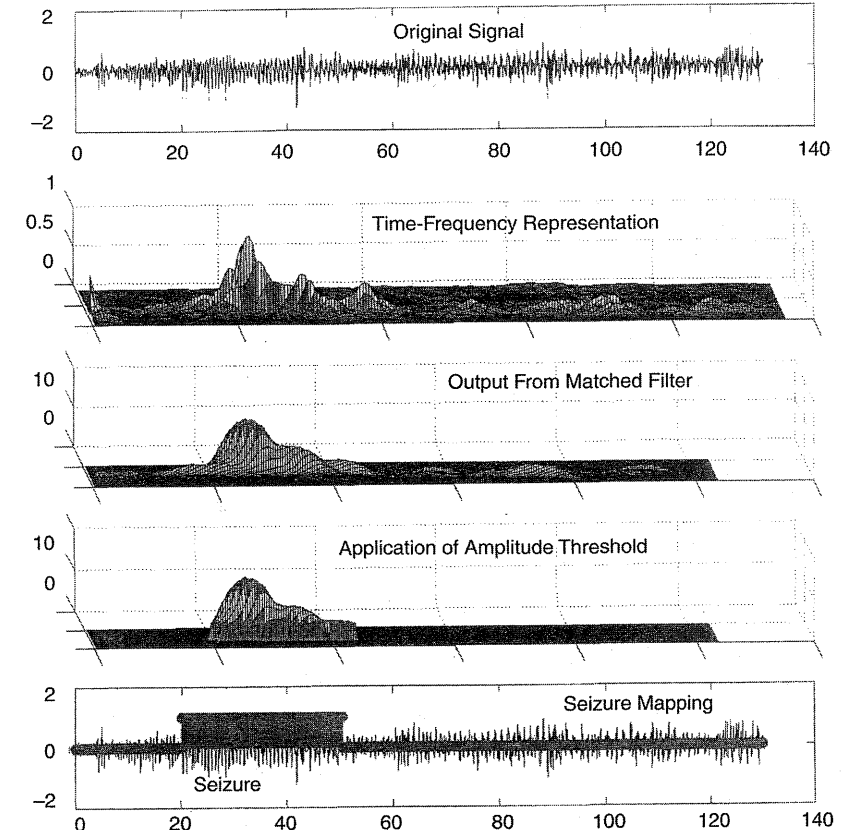


FIGURE 9.23
Different steps of seizure localization.

9.5.1.6 Map seizure decision to real-time location

This stage simply ties all the independent decisions on each block of processed signal (remapping any seizure decision to a time series function) of equivalent length to the input EEG signal. This output waveform consists of ones or zeros, where one indicates the presence of seizure at the corresponding time. Figure 9.23 summarizes the five stages from input signal to seizure indicated on the output signal.

9.5.2 Experimental setup

To validate and calibrate the detection method, simulated data generated by the EEG model proposed by Roessgen, Zoubir and Boashash [28] is used.

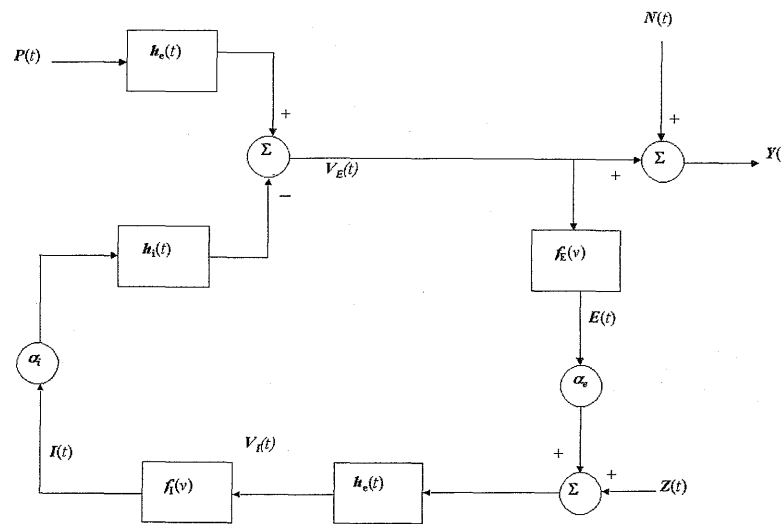


FIGURE 9.24
EEG model.

9.5.2.1 Electroencephalogram model

Roessgen extended the model of the α rhythm of the thalamus proposed by da Silva [22] by introducing a seizure input waveform $Z(t)$ as shown in Figure 9.24. The model considers a population of interconnected neurons driven by a random input — a WGN $P(t)$ — that is assumed to originate from deeper brain structure such as thalamus and brain stem. The parameters of the model reflect some physiological characteristics such as neuronal interconnectivity, synaptic pulse response and excitation threshold. For an in-depth discussion of this model, see [28].

To account for the nonstationarities of the EEG, the periodic sawtooth signal $Z(t)$ of period f_c used by Roessgen was replaced by the following more realistic quasi-periodic nonstationary signal that fits a linear FM law with a time-varying amplitude:

$$S_{LFM}(t) = Z(t)e^{j\pi\alpha t^2} \quad (9.15)$$

The typical range for α is $[-0.07$ to $0]$. The initial frequency f_0 is typically in the range of 0.5 to 5 Hz. These values were reported in [15, 21]. A signal-to-background ratio (SBR) was introduced to account for the fact that the seizure and background components of the newborn EEG are of almost similar magnitudes. The SBR in decibels is defined as:

$$SBR = 10 \log \left(\frac{\sigma_s^2}{\sigma_b^2} \right) \quad (9.16)$$

where σ_s^2 and σ_b^2 represent the power in the seizure and the background components of the EEG signal, respectively.

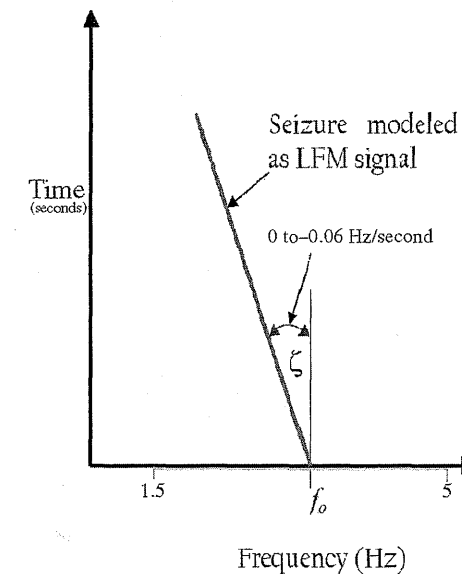


FIGURE 9.25
Template model.

9.5.2.2 Template selection

The reference template to be used for detection is the TF distribution of a linear FM (LFM, Figure 9.25). The duration of the LFM signal is set at 20 sec as discussed earlier. We have chosen the slope of the LFM to be negative because the majority of the seizures encountered at this stage are characterized by a frequency that is either constant or decreasing with time.

To find the best slope of the template ridge (see Figure 9.25), that is, the one that corresponds to the best detection rate for the different types of seizures, a testing stage was necessary. A number of templates with different ridge slopes were created. These templates were tested using the seizure detection system presented earlier (see Figure 9.20) and a number of EEG signals produced by the model in Figure 9.24. These signals were generated using different combinations of the model parameters. It was found that the template with $\zeta = -0.05$ Hz/sec gives the best results.

9.5.2.3 Threshold selection

To select an optimum threshold that realizes the good compromise between the rate of good detections and the rate of false alarms, a similar test to the one previously discussed was performed. Among the different thresholds tested, the ones that have a value around 4 resulted in a good compromise.

9.5.3 Time-frequency detector evaluation

To check its reliability and to validate its effectiveness, the TF detector is tested using synthetic data generated by the EEG model (see Figure 9.24). The synthetic signal contains a mixture of randomly placed seizures and background. For this investigation, 1000 synthetic EEG signals were used, with the parameter selection varied as follows:

- SBR = random [0 to 20 dB]
- SNR = random [0 to 20 dB]
- α = random [-0.06 to 0]
- f_c = random [1.5 to -5]

The average detection rate was 99.1 whereas the false alarm rate was 0.4%. These good results were expected because the template adopted is well adapted to the EEG model that only produces noisy linear FM signals with time-varying amplitudes. Other EEG models could be able to generate different types of EEG-like seizures such as piecewise LFM. For those signals, a template such as the one proposed by Celka, Boashash and Colditz [11] would be used.

9.6 Discussion and Conclusions

This chapter shows that the TF domain is the preferable basis from which to develop a complete EEG seizure detection scheme. The proposed TF approach was successfully calibrated using existing methods based on autocorrelation detection criteria and spectral estimation methods

The initial patterns obtained by a TF analysis of EEG seizure signals specifically confirm that EEG seizures in newborn are well characterized by a linear FM or piecewise linear FMs. These results are encouraging and further analysis on other data sets is currently in progress to refine and extend these findings. The characterization of nonstationary EEG signals in the TF domain is the first step toward an automatic method of seizure detection and classification that use powerful tools of TF signal processing [6]. In this direction and based on the findings thus far obtained, we proposed a TF detector based on cross-correlating the TF representation of the EEG signal with a TF reference template. The design of the template takes into account the TF characteristics of the EEG seizure thus far extracted. The performance of this TF detector was tested on synthetic signals. The results obtained were very encouraging (99.1% detection rate and 0.4% false alarm rate). Current work not yet finalized at time of publication is concentrating on using real newborn EEG signals.

Acknowledgments

This work is funded by the Australian Research Council (ARC). The authors wish to thank Professor Paul Colditz of the Royal Women's Hospital in Brisbane for providing us access to the Perinatal Research Centre and Dr. Chris Burke of the Royal Children Hospital for the interpretation of the EEG data.

References

- [1] R.A. Altes, Detection, estimation, and classification with spectrogram, *J. Acoust. Soc. Am.*, 67(4), 1232–1246, April 1980.
- [2] B. Boashash and P. O'Shea, Time-Frequency Analysis Applied to Signaturing of Underwater Acoustic Signals, International Conference of Acoustics, Speech, and Signal Processing, New York, April 11–14, 1988.
- [3] B. Boashash and P. O'Shea, Application of Wigner–Ville distribution to the identification of machine noise, in Proceedings of the SPIE, 975, 209–220, August 1988.
- [4] B. Boashash and P. O'Shea, A methodology for detection and classification of some underwater acoustic signals using Time-Frequency analysis techniques, *IEEE Trans. ASSP*, 38(11), 1829–1844, November 1990.
- [5] B. Boashash, Time-Frequency signal analysis, in S. Haykin, Ed., *Advances in Spectral Estimation and Array Processing*, Prentice Hall, New York, 1991, pp. 418–517.
- [6] B. Boashash, Ed., *Time-Frequency Signal Analysis: Methods and Applications*, Longman Cheshire/Wiley, Melbourne/New York, 1992.
- [7] B. Boashash and V. Sucic, A Resolution Performance Measure for Quadratic Time-Frequency Distributions, in Proceedings of the IEEE Workshop on Statistical Signal and Array Processing, Pocono Manor, PA, 2000, pp. 584–588.
- [8] B. Boashash, H. Carson, and M. Mesbah, Detection of Seizures in Newborns Using Time-Frequency Analysis of EEG Signals, in Proceedings of the IEEE Workshop on Statistical Signal and Array Processing, Pocono Manor, PA, 2000, pp. 564–568.
- [9] B. Boashash, M. Mesbah, and P. Colditz, Newborn EEG Seizure Pattern Characterization Using Time-Frequency Analysis, in Proceedings of the International Conference on Acoustics, Speech, and Signal Processing (on CDROM), Salt Lake City, UT, May 2001.

- [10] B. Boashash and M. Mesbah, A Time-Frequency approach for newborn seizure detection: rationale and relationship to stationary methods, *IEEE Eng. Med. Biol. Mag.* [in press].
- [11] P. Celka, B. Boashash, and P. Colditz, Pre-processing and Time-Frequency analysis of newborn EEG seizures, *IEEE Eng. Med. Biol. Mag.*, [in press].
- [12] R. Clancy, Interictal sharp EEG transients in neonatal seizures, *J. Child Neurol.*, 4, 30–38, 1989.
- [13] P. Flandrin, A Time-Frequency formulation of optimum detection, *IEEE Trans. Acoust. Speech Signal Process.*, 36(9), September 1988.
- [14] P.J. Franaszczuk, G.K. Bergy, P.J. Durka, and H.M. Eisenberg, Time-Frequency analysis using matching pursuit algorithm applied to seizure originating from the mesial temporal lobe, *Electroencephalogr. Clin. Neurophysiol.*, 106, 513–521, 1998.
- [15] J. Gotman, J. Zhang, J. Rosenblatt, and R. Gotman, Automatic seizure detection in newborns and infants, in Proceedings of the IEEE Engineering in Medicine and Biology Society, 2, 913–914, 1995.
- [16] J. Gotman, J. Zhang, J. Rosenblatt, and R. Gottesman, Evaluation of an automatic seizure detection method for the newborn EEG, *Electroencephalogr. Clin. Neurophysiol.*, 103, 363–369, 1997.
- [17] A.J.E.M. Janssen, Positivity and spread of Time-Frequency distributions, in *The Wigner Distribution: Theory and Applications in Signal Processing*, W. Meclenbrauker and F. Hlawatsch, Eds., Elsevier, Amsterdam, 1997, pp. 1–58.
- [18] S. Kay and G.F. Boudreux-Bartels, On the Optimality of the Wigner Distribution for Detection, in Proceedings IEEE International Conference on Acoustics, Speech, and Signal Processing, March 1985, pp. 1017–1020.
- [19] P. Kellaway and R.A. Hratchovy, Status epilepticus in newborns: a perspective on neonatal seizures, in *Advances of Neurology*, A.V. Delgado-Escueta, C.G. Wasterlain, D.M. Treiman, and R.J. Porter, Eds., Vol. 34, Raven Press, New York, 1983, pp. 93–99.
- [20] A. Liu, J.S. Hahn, G.P. Heldt, and R.W. Coen, Detection of Neonatal Seizures through Computerized EEG Analysis, *Electroencephalogr. Clin. Neurophysiol.*, 82, 30–37, 1992.
- [21] C.T. Lombroso, Neonatal EEG polygraphy in normal and abnormal newborns, in *Electroencephalography: Basic Principles, Clinical Applications, and Related Fields*, E. Niedermeyer and F.H. Lopes da Silva, Eds., Williams & Wilkins, Baltimore, 1993, pp. 802–875.
- [22] F.H. Lopes da Silva, Dynamics of EEG as signals of neuronal population: models and theoretical considerations, in *Electroencephalography: Basic*

- Principles, Clinical Applications, and Related Fields*, E. Niedermeyer and F.H. Lopes da Silva, Eds., Williams & Wilkins, Baltimore, 1993.
- [23] C.N. McCutchen, R. Coen, and V.J. Iragui, Periodic lateralized epileptiform discharges in asphyxiated neonates, *Electroencephalogr. Clin. Neurophysiol.*, 61, 210–217, 1985.
- [24] M. Mesbah, B. Boashash, and P. Colditz, Analysis of Newborn EEG Time-Frequency Patterns, in Proceedings of the 3rd Australian Workshop on Signal Processing and its Applications (on CDROM), Brisbane, Australia, December 2000.
- [25] A.J. Olievera, M.L. Nunes, and J.C. da Costa, Polysomnography in neonatal seizures, *Clinical Neurophysiol.*, 111, Suppl. 2, S74–S80, 2000.
- [26] A. Papandreou, S. Kay, and G. Faye Boudreux-Bartels, The use of Hyperbolic Time-Frequency Representations for Optimum Detection and Parameter Estimation of Hyperbolic Chirps, in Proceedings of the IEEE-SP International Symposium on Time-Frequency and Time-Scale Analysis, Philadelphia, October 25–28, 1994, pp. 369–372.
- [27] A. Papandreou, G.F. Boudreux-Bartels, and S.M. Kay, Detection and estimation of generalized chirps using Time-Frequency representations, in 28th Annual Asilomar Conference on Signals, Systems and Computers, Pacific Grove, CA, November 1994, pp. 50–54.
- [28] M. Roessgen, A. Zoubir, and B. Boashash, Seizure detection of newborn EEG using a model based approach, *IEEE Trans. Biomed. Eng.*, 45(6), June 1998.
- [29] J.C. Rowe, G.L. Holmes, J. Hafford, S. Robinson, A. Philipps, T. Rosenkrantz, and J. Raye, Prognostic value of the electroencephalogram in term and preterm infants following neonatal seizures, *Electroencephalogr. Clin. Neurophysiol.*, 60, 183–196, 1985.
- [30] B. Samimi and G. Rizzoni, Time-Frequency Analysis for Improved Detection of Internal Combustion Engine Knock, in Proceedings of the IEEE-SP International Symposium on Time-Frequency and Time-Scale Analysis, Philadelphia, October 25–28, 1994, pp. 178–181.
- [31] L.L. Scharf, *Statistical Signal Processing — Detection, Estimation, and Time Series Analysis*, Addison-Wesley, Reading, MA, 1991.
- [32] H.L. Van Trees, *Detection, Estimation, and Modulation Theory*, John Wiley & Sons, New York, 1968.
- [33] S.P. Varma, A. Papandreou-Suppappola, and S.B. Suppappola, Detecting Faults in Structures Using Time-Frequency Techniques, in Proceedings of the IEEE International Conference on Acoustics, Speech, and Signal Processing (on CDROM), Salt Lake City, UT, May 2001.
- [34] J.J. Volpe, Neonatal seizures, in *Neurology of the Newborn*, W.B. Saunders, Philadelphia, 1995, pp. 172–207.